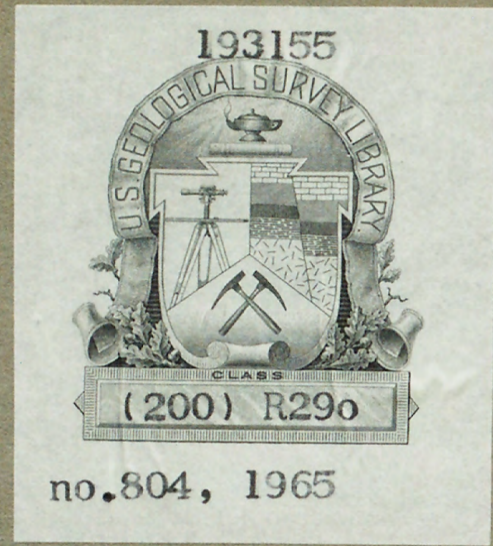


U. S. Geological Survey:

REPORTS-OPEN FILE SERIES, no. 804: 1965.



(200)
R29o



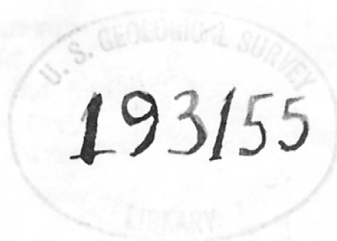
(200)

R290

no. 804

✓
U. S. Geological Survey.

Reports - open file series, no. 804; 1965]



12 JUL 1965

(200)
R290.
no. 804

U. S. Geological Survey.
[Reports - Open file series, no. 804]

USGS LIBRARY - RESTON



ALLANITES FROM THE BOULDER CREEK

BATHOLITH, COLORADO

For further information concerning open files, the following
copies are available at the Geological Survey Library, 1833 3rd
Washington, D. C., and other offices as listed:

Nelson Lawson Hickling, 10th, Colorado, by Nelson
Hickling, Jr., Federal Bldg., Denver, Colo., 80202, U.S. Library,
Bldg. 25, Federal Bldg., Denver, Colo., 80202.

Stratigraphy of the Mobil Oil Company Paleozoic test well
No. 22-1-A, tip-top map, Sweetwater County, Wyoming, by John F. Harald
29 pp., sheets of core descriptions, file 22-1-A, Federal Bldg., Denver,
Colo., 80202, Federal Bldg., Denver, Colo., 80202, U.S. Library,
Salt Lake City, Utah 84105, Federal Bldg., Denver, Colo., 80202,
Boulder Park, Colo. Copy from which reproduction
expenses are available in all depositories.



Additional depositories as shown are hereby designated for the
following reports which were announced on July 2, 1965:

Geological Survey, Denver, Colo., 80202, U.S. Library,
Bldg. 25, Federal Bldg., Denver, Colo., 80202.

Preliminary geological map, U. S. Geological Survey
W. P. Bunting and R. E. Bunting, 10th, Colorado, Alaska, by
OPEN FILE REPORT

This report is preliminary and has
not been edited or reviewed for
conformity with Geological Survey
standards or nomenclature.

accompanying
(200)
R 29a
no 204 Weld - Int. 2905

GEOLOGIC DIVISION
U. S. GEOLOGICAL SURVEY
Washington, D. C.

For release JULY 9, 1965

The U. S. Geological Survey is releasing in open files the following reports. Copies are available in the Geological Survey Library, 1033 GSA Bldg., Washington, D. C., and in other offices as listed:

1. Allanites from the Boulder Creek Batholith, Colorado, by Nelson Lawson Hickling. 48 p., 2 pl., 20 figs., 6 tables. USGS Library, Bldg. 25, Federal Center, Denver, Colo.
2. Stratigraphy of the Mobil Oil Company Paleozoic test well No. 22-19-G, Tip-top unit, Sublette County, Wyoming, by John E. Marzolf. 39 p., 2 sheets of core descriptions. Bldg. 25, Federal Center, Denver, Colo.; 15426 Federal Bldg., Denver, Colo.; 8102 Federal Office Bldg., Salt Lake City, Utah; 305 Federal Bldg., Casper, Wyo.; 345 Middlefield Rd., Menlo Park, Calif. Copy from which reproduction can be made at private expense is available in all depositories.

* * * * *

Additional depositories as shown are hereby designated for the following reports which were announced on July 2, 1965:

Geologic map and cross sections of the Nelchina area, south-central Alaska, by Arthur Grantz.

Preliminary geologic map of the Arctic quadrangle, Alaska, by W. P. Brosigé and H. N. Reiser.

Office of the State Geologist, 404 State Capitol Bldg., Juneau, and 800 L St., Anchorage, Alaska.

* * * * *

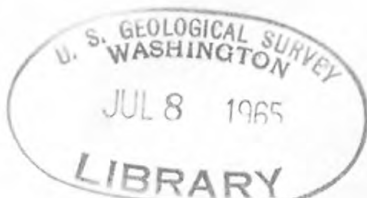


TABLE OF CONTENTS

	PAGE
INTRODUCTION	1
GEOLOGIC SETTING	3
LABORATORY METHODS	5
Separations	5
Optical Methods	6
X-ray L-spacing	9
Chemical Data	9
DISCUSSION OF DATA.....	11
METAMICHTIZATION	26
PARAGENESIS OF ALLANITE AND EPIDOTE	40
SUMMARY AND CONCLUSIONS	43
ACKNOWLEDGEMENTS	46
BIBLIOGRAPHY	47

LIST OF TABLES

TABLE	PAGE
1 Optics for Allanites from the Boulder Creek	8
Batholith	8
2 Calculated and Measured D-spacings for Allanite ...	
Sample 1	10
3 X-ray Fluorescence Analysis of Allanites from	
the Boulder Creek Batholith	12
4 Fluorimetric Uranium and Thorium Determinations ...	
on Allanites from the Boulder Creek Batholith ...	13
5 Microanalysis of Allanites from the Boulder	
Creek Batholith	14
6 Summation for Allanite Compositions	15

LIST OF ILLUSTRATIONS

FIGURE	PAGE
1. Plot of Beta Index for Allanite against Fe_2O_3 Content of Allanite:	16
2. Plot of Beta Index for Allanite against FeO/Fe_2O_3 Ratio for Allanite	17
3. Plot of Beta Index for Allanite against CeO_2 Content of Allanite	19
4. Plot of Beta Index for Allanite against La_2O_3 Content of Allanite	19
5. Plot of Beta Index for Allanite against Nd_2O_3 Content of Allanite	20
6. Plot of Beta Index for Allanite against the Sum $CeO_2 + Nd_2O_3 + Fe_2O_3$ in Allanite	21
7. Plot of CeO_2 Content of Allanite against SiO_2 Content for Bulk Rock	23
8. Plot of La_2O_3 Content of Allanite against SiO_2 Content for Bulk Rock	24
9. Plot of Nd_2O_3 Content of Allanite against SiO_2 Content for Bulk Rock	24
10. Total Rare-earth Oxide Content of Allanite Plotted against SiO_2 Content for Bulk Rock	25
11. Combined Plot Showing Individual Rare-earth Oxides from Allanite Recalculated to 100% and Plotted as to Rock Type	27
12. ThO_2 Content of Allanite Plotted against Birefringence of Allanite	30

LIST OF ILLUSTRATIONS

FIGURE	PAGE
13. U + $\frac{1}{2}$ Th Content of Allanites in Parts Per Thousand Plotted against Birefringence of Allanite .	30
14. Beta Index for Allanite Plotted against Birefringence of Allanite	31
15. Combined Plots of Alpha, Beta, and Gamma Indices for Allanite against Expanded Scale of Birefringence for Allanite	33
16. U Content of Allanites Plotted against SiO ₂ Content for Bulk Rock	35
17. ThO ₂ Content of Allanites Plotted against SiO ₂ Content for Bulk Rock	36
18. Plot of Th Content of Allanite in Parts Per Thousand against the Lime-alkali Ratio of Bulk Rock	37
19. Plot of Thorium Content of Allanite against Th/U Ratio for Allanite	38
20. Plot of U Content of Allanites against Th/U Ratio for Allanite	39

PLATE

1. Outline map of the Boulder Creek Batholith with Sample Locations	2
2. Sketches of Allanite and Epidote and Associated Minerals as Observed in Thin Section	41

Introduction

Allanite is the rare earth member of the epidote group of minerals with composition generally expressed as $(\text{Ca},\text{Ce})_2(\text{Fe}^{2+},\text{Fe}^{3+})\text{Al}_2\text{O}_5\text{OH}(\text{Si}_2\text{O}_7)(\text{SiO}_4)$ ^{1/}. Although there have been several investigations of allanite in pegmatites, studies of allanite from granitoid rocks to date are rare.

This study of accessory allanites from the Boulder Creek batholith is an adjunct to the comprehensive petrologic study of that batholith by George Phair and David Gottfried of the U. S. Geological Survey. The allanites studied represent a suite of twenty rocks systematically collected from the Precambrian Boulder Creek batholith which intrudes gneisses and schists of the older Precambrian Idaho Springs formation. Plate 1 shows the sample locations of the twenty allanite concentrates studied and the geologic setting of their host rocks. Allanite is unusually abundant in these rocks and occurs as crystals and/or irregular aggregates ranging from a fraction of a millimeter to a centimeter in maximum dimension. Unlike most pegmatitic allanites these are only partially metamict, thus making it possible to obtain complete optical and X-ray data.

From the observed relationship between the indices of refraction, d-spacings and chemical composition, it is possible to evaluate the role of allanite in the incorporation of radioactive elements, such as uranium and thorium, and how the

^{1/} Deer, W. A., Howie, R. A., and Zussman, J., 1962, Rock Forming Minerals. New York: John Wiley and Sons, Inc., vol. 1, p. 211.

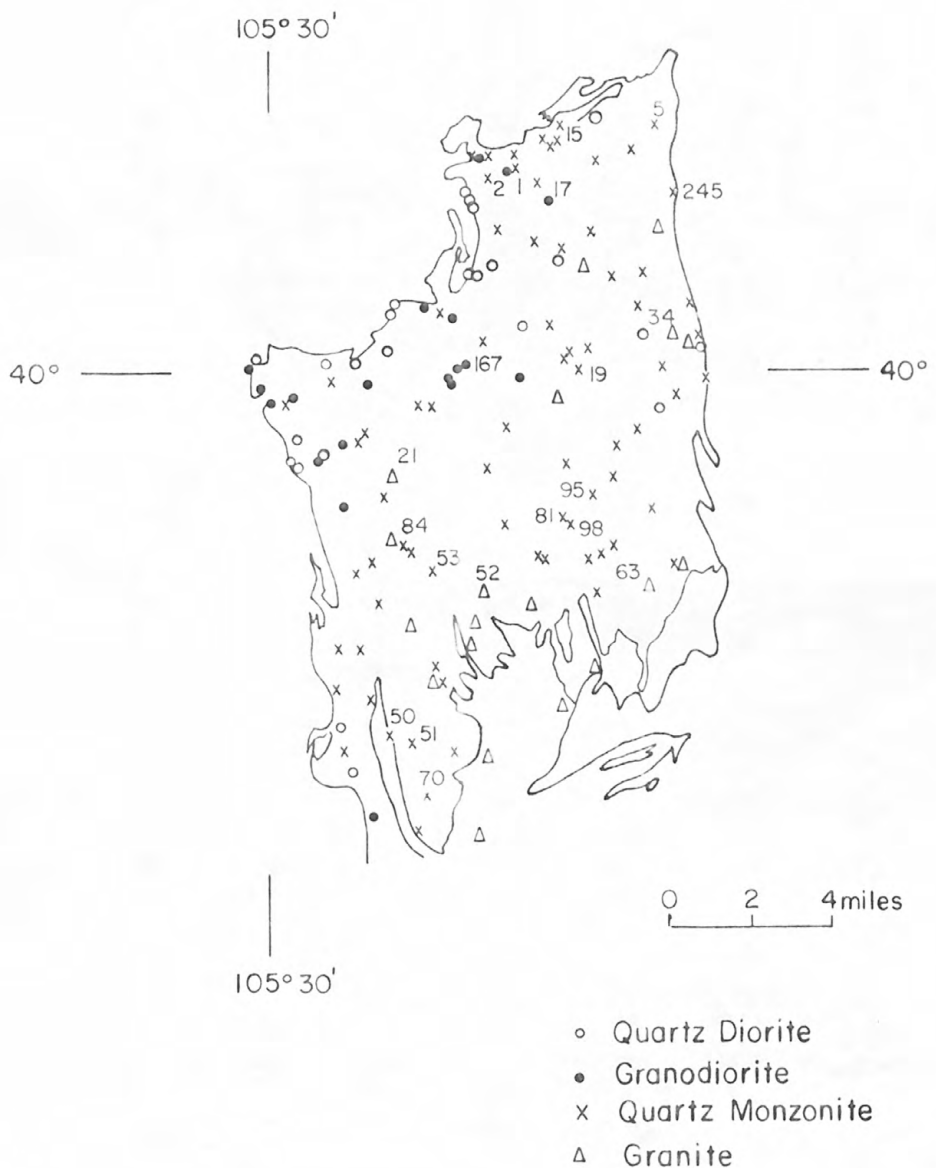


Plate I Outline map of the Boulder Creek batholith
 showing sample locations. (After G. Phair and D. Gottfried, 1964)
 Based on data from

decay of these elements bear on the problem of metamictization. Moreover, the data here presented furnish additional information as to the distribution of the rare earths (Ce, La, Nd, Sm and Cd) in alienite.

Geologic Setting

The Boulder Creek batholith is west of Boulder, Colorado, in the central portion of the Colorado Front Range. The study of this batholith has been important because of its close association ~~with~~ ^{with} the Front Range Mineral Belt which is thought to be of Laramide age.

The brief geologic description presented here is drawn mainly from the work of Lovering and Goddard, 1950, and ^{2/} unpublished work by Phair and Gottfried.

The rocks of the Front Range consist of a series of Precambrian batholiths and stocks of granitic composition ^{intrusive} ~~into~~ earlier Precambrian sediments which were consequently deformed and metamorphosed. The exposed rocks of the Front Range are thus divided into two groupings: the Precambrian granitic batholiths and stocks and the metasediments of earlier Precambrian age which have been intruded and deformed so that they nearly everywhere surround and interfinger between the various batholiths.

^{2/} Lovering, T. S., and Goddard, E. N., 1950, "Geology and Ore Deposits of the Front Range Colorado", U. S. Geological Survey Professional Paper 223, 319 pp.

The older Precambrian metamorphics are at least 1700 million years old and consist of gneiss, gneissic aplite, schists, pegmatites and lesser quantities of quartzites and pebble conglomerate. The later Precambrian granitic rocks are generally grouped as the Boulder Creek granite (1700 m.y.), the Silver Plume granite (1400 m.y.)^{3/} and the Pikes Peak granite (1000 m.y.).^{4/} The Boulder Creek granite is the oldest and least abundant of the three. It is usually distinguished in the field by its dark-gray color and its faint banding. The Pikes Peak granite is very pink and usually coarser grained and the Silver Plume is fine grained and has a light pinkish-gray color.

The Boulder Creek batholith is the largest single body of Boulder Creek granite in the Front Range. It is approximately twenty miles long in a north-south direction and eleven miles wide in an east-west direction. It is seen from Plate 1 that the term Boulder Creek granite includes a variety of rock types. The Boulder Creek batholith lies immediately south of the northeast end of the Front Range Mineral Belt. The main trend of the mineral belt begins near Breckenridge, Colorado, on the western border of the Front Range and traces a direction of N 35° E for

^{3/} Stern, T., Rhair, G., and Gottfried, D., unpublished data.

^{4/} Davis, G. L., Tilton, G. R., Aldrich, L. T., Wetherill, G. W., and Paul, H., 1957, "The Age of Rocks and Minerals", Annual Report of the Director of the Geophysical Laboratory, Carnegie Institution of Washington, No. 1277, p. 166.

^{5/} Davis, G. L., Aldrich, L. T., Tilton, G. R., Wetherill, G. W., and Jeffery, P. M., 1956, "The Age of Rocks and Minerals", Annual Report of the Director of the Geophysical Laboratory, Carnegie Institution of Washington, No. 1265, p. 165.

approximately fifty five miles ending a few miles northwest of Boulder, Colorado on the eastern border of the Front Range. This trend is outlined by a series of Laramide intrusive stocks and smaller hypabyssal bodies as well as the Laramide dikes and veins associated with them. The Laramide intrusive stocks are generally intruded into a zone of older Precambrian metasediments which lie between major later Precambrian igneous batholiths of granitic composition. The Laramide dikes and veins commonly trend across both metamorphic and igneous terrane. The reader is referred to the work by George Phair and Francis Fisher in 6/ 1962 for a detailed comprehensive study and classification of this Laramide series of rocks.

Laboratory Methods

Separation

Twenty to thirty pounds of rock for each sample were crushed and sieved. The portion in the 100-200 mesh size was then used in the further separations. Appropriate heavy liquids were used in order of increasing densities in order to keep the allanite in the heavier fractions and in the meantime floating out increasing amounts of the lighter heavy mineral suite. The order of use and the ^{specific gravities} of the heavy liquids used were:

6/ Phair, G., and Fisher, F. G., 1962, "Laramide Comagmatic Series in the Colorado Front Range: The Feldspars", Petrologic Studies: A Volume to Honor A. F. Buddington, Geol. Soc. Am., pp. 479-522.

1. bromoform (2.89)
2. methylene iodide (3.3)
3. clerici solution (3.4)
4. clerici solution (3.54) and
5. clerici solution (> 4.005).

Generally, at least, 80% of the allanites remained in the progressively denser heavy fractions until the last clerici solution with density > 4.005 was used. Here most of the allanite plus some epidote and sphene floated. The portion then with gravity > 3.54 and less than the liquid with a gravity of a little more than 4.005 was washed repeatedly with large volumes of warm distilled water to completely remove any traces of thallium from the clerici solution (thallous formate + thallous malonate).

Most of the sphene and epidote were removed from the concentrate on a Frantz magnetic separator. The bulk of the allanite was obtained at amperage settings varying from $0.4\frac{1}{4}$ - $0.4\frac{3}{4}$, when a tilt of 12° and a slope of 20° was used. The concentrates were then hand picked to achieve a purity of at least 98% allanite in all cases. What impurity was left if any consisted of scattered partial rims of epidote which could not be separated from the allanite in an ultrasonic disaggregator.

Optical Methods

Because of the very small initial amounts of allanite concentrated, optics were determined by mounting single grains on the tip of a spindle stage designed and described by

R.E.

1/

Wilcox, U. S. G. S. For each sample six separate grains were mounted, in turn, and the three principle directions (α , β , γ) of index of refraction were then measured on each individual grain.

The average of these six determinations is used here as the indices of refraction for each particular sample. In cases where suitable interference figures could not be found to use in finding the optical orientations for the principle directions of index of refraction, the orthoscopic procedure described by Wilcox was used. For all determinations made the matching index oil was checked on a Leitz-Jelly refractometer. The indices obtained for sample 245 are not representative of the entire sample but are *the best that could be obtained.*

1/ ~~Optical~~ Optical determinations on the majority of the grains were not possible due to the very dark color and a network of cracks and hackly relief which combined to so disperse the light that following the movement of a becke line was impossible. The six grains used were not very fresh and were of a lighter color representing only about 30% of the sample. If optics could have been determined they would have been close to the average for this allanite suite. Table 1 shows the optical data for the allanites.

1/ Wilcox, R. E., 1959, "Use of Spindle Stage For Determining Refractive Indices of Crystal Fragments", American Mineralogist, vol. 44, pp. 1272-1293.

Table 1

Optics for allanites from the Boulder Creek batholith

Sample No.	α	β	γ	$\gamma-\alpha$	est. 2V	Calc. 2V	Optic sign
GP - 1	1.752	1.771	1.784	.032	--	78°	-
GP - 2	1.745	1.761	1.771	.026	50°-60°	76°	-
GP - 5	1.726	1.740	1.750	.024	60°-70°	80°	-
GP - 15	1.745	1.765	1.776	.031	--	72°	-
GP - 17	1.734	1.749	1.759	.025	--	71°	-
GP - 19	1.726	1.739	1.748	.022	--	79°	-
GP - 21	1.759	1.774	1.782	.023	--	72°	-
GP - 34	1.728	1.744	1.752	.024	70°	70°	-
GP - 50	1.751	1.762	1.771	.020	70°	84°	-
GP - 51	1.747	1.760	1.767	.020	--	72°	-
GP - 52	1.747	1.761	1.770	.023	70°	77°	-
GP - 53	1.752	1.766	1.773	.021	70°	70°	-
GP - 63	1.740	1.756	1.766	.026	--	76°	-
GP - 70	1.731	1.744	1.754	.023	70°	82°	-
GP - 81	1.744	1.759	1.768	.024	65°-75°	75°	-
GP - 84	1.756	1.769	1.778	.022	70°	79°	-
GP - 95	1.748	1.764	1.775	.027	70°-75°	79°	-
GP - 98	1.750	1.763	1.773	.023	--	82°	-
GP - 167	1.749	1.766	1.776	.027	70°	74°	-
GP - 245	1.719	1.731	1.741	.022	--	84°	-

Pleochroism strong.

X = pale tan to light brown
 Y = very dark reddish brown,
 occasionally greenish brown
 Z = dark brown
 X << Z < Y

X-ray d-spacings

D-spacings have been determined for all of these allanites and they match very closely those given in the A.S.T.M. X-ray index file for fresh allanite. The allanites of lower indices of refraction have d-spacings very nearly the same as those for the allanites of the highest indices of refraction, but the lines on the film for the samples with low optics were much broader and less distinct than for the others. Several of these had to be run six or more times at different settings and varying lengths of time in order to obtain a pattern that would meet even minimum standards of line definition for accurate measurements. A powder camera was used on the weak port of a copper radiation source with a nickel filter. Because back reflections were usually absent, a camera with a film stop that could be turned 45° from the usual position was used so that a portion of the strong front lines could be exposed on the other end of the film permitting to film shrinkage to be measured. D-spacing measurements for these allanites are quite uniform. Sample 1 has been indexed, as the measured d-spacings would show it to fall midway in the small range of variation in d-spacings for these allanites. The data for sample 1 is shown in Table 2, and can be considered representative for the allanite suite.

Chemical Data

Because of the small initial size of these allanite concentrates only those analyses not requiring large amounts of sample could be made. Several of the samples were so small as to

Table 2

Calculated and measured d-spacings for allanite sample 1

Calculated			Measured		Calculated			Measured	
h _k l	d _{hkl}	I	d _{hkl}		h _k l	d _{hkl}	I	d _{hkl}	
001	9.23	4	9.24		10 ⁴	2.520			
100	8.15				121	2.506			
101	8.04	4	8.03		122	2.496	1	2.494	
010	5.74				310	2.456			
101	5.13	2	5.12		022	2.439			
102	5.04	3	5.04		31 ³	2.428			
011	4.878	1	4.890		221	2.422	2	2.416	
110	4.697				301	2.350			
111	4.673	4	4.673		220	2.348			
002	4.617				212	2.340			
201	4.502	1	4.507		222	2.337	2	2.336	
200	4.075				113	2.326			
202	4.019	2	4.024		30 ³	2.309			
111	3.824	2	3.806		004	2.308			
112	3.789				214	2.308	2	2.307	
012	3.600	1	3.601		114	2.308			
211	3.544	8	3.528		402	2.252	1	2.249	
102	3.439				122	2.204			
103	3.397				401	2.196			
210	3.324	3	3.324		12 ²	2.193	2	2.189	
212	3.294				403	2.178			
201	3.253	1	3.239		511	2.173			
203	3.195				221	2.153	3	2.149	
003	3.078				314	2.143			
301	2.971				014	2.142			
302	2.955				223	2.136			
112	2.951				023	2.100	1	2.104	
113	2.923	10	2.922		203	2.069	1	2.058	
020	2.872	4	2.868		205	2.039			
211	2.850	4	2.819		400	2.038			
213	2.792				404	2.009			
021	2.743				104	2.008	2	2.003	
300	2.717				302	1.999			
013	2.713				105	1.993			
120	2.709				520	1.974			
121	2.705	8	2.706		303	1.964			
302	2.679				213	1.947			
311	2.639				215	1.922	1	1.921	
312	2.627	7	2.625		030	1.915			
202	2.563	5	2.554		222	1.912			
103	2.545				123	1.904			
204	2.521				114	1.896	2	1.898	

d_{hkl} calculated from the following data: a = 9.05 ± .04 Å,
 b = 5.74 ± .02 Å, c = 10.26 ± .04 Å and $\beta = 115^{\circ}10' \pm 15'$. Film
 shrinkage negligible. All calculated d-spacings listed for $d \geq 1.896$.

allow only optical and X-ray work. Others were large enough to have thirteen major and minor elements determined by X-ray fluorescence analysis with enough sample left for determination of FeO, MgO, and H₂O by microanalytical techniques. Thirteen samples were analyzed by ^{chemically} ^{highly sensitive and} ~~precise~~ techniques for determination of uranium and thorium.

Tables 3, 4, and 5 show the results of these chemical determinations. Table 6 shows the summations for the compositions of these allanites when the chemical data are combined.

Discussion of Data

It should be remembered when relationships are discussed or shown on plotted diagrams the total number of samples involved will vary from one set of parameters to another depending on the number of allanites analyzed for those components. In those cases where definite trends are established a solid line will be used; when only a general trend appears a dashed line will be used and in equivocal cases where only a field or fields of relationships result these will be distinguished by appropriately placed dashed line borders.

Figure 1 shows a plot of β_{N} against the Fe₂O₃ content of six samples of allanite, which shows β_{N} increasing with increasing Fe₂O₃ content. Figure 2 shows a decrease in β_{N} when plotted against increasing FeO/Fe₂O₃ ratio for the same six samples. Commonly the refractive indices of a mineral increase with increasing iron content, but when the β_{N} for these allanites are plotted against total iron a complete scatter of

Table 5

X-ray fluorescence analysis of allanites from
the Boulder Creek batholith*

Sample No.	15	17	21	54	51	52	167	245
SiO ₂	30.0	29.5	30.4	28.0	29.8	30.6	30.8	30.4
Al ₂ O ₃	14.5	14.7	15.1	14.3	14.0	14.5	14.6	14.4
Fe ₂ O ₃ (total)	18.3	16.3	17.0	17.5	14.1	13.6	16.1	16.3
CaO	12.7	13.9	13.3	13.5	11.7	12.4	13.8	13.2
MnO	0.45	0.50	0.46	1.02	0.35	0.7	0.4	0.70
TiO ₂	0.92	0.56	0.77	0.86	1.03	0.88	0.60	0.87
CeO ₂	8.8	9.3	10.5	8.3	8.8	10.8	9.7	9.8
La ₂ O ₃	4.6	4.7	5.1	5.4	4.1	5.0	4.3	4.6
Nd ₂ O ₃	2.4	2.7	3.0	2.3	2.6	3.1	2.8	3.0
Sm ₂ O ₃	0.65	0.68	0.73	0.65	0.70	1.3	1.2	.72
Gd ₂ O ₃	0.50	0.52	0.62	0.61	0.48	0.6	0.5	0.56
Y ₂ O ₃	< .1	< .1	< .1	0.2	< .1	< .1	< .1	0.2
ThO ₂	0.41	0.62	0.62	1.8	1.0	1.5	1.1	1.5

* Analysts Harry Rose and Robena Brown -- U. S. Geological Survey.

Table 4

Fluorimetric Uranium and Thorium determinations on allanites
from the Boulder Creek batholith*

Sample No.	U ppm	Th ppm
2	82	4,965
5	84	10,897
15	54	4,965
17	107	5,317
21	70	6,723
51	158	11,380
52	140	9,755
53	138	9,623
84	146	9,403
95	148	9,447
98	122	10,633
167	146	10,194
245	102	11,600

* Analyst Roosevelt Moore -- U. S. Geological Survey.

Table 5

 Microanalysis of allanites from
 the Boulder Creek batholith*

Sample No.	% FeO	% MgO	% H ₂ O+	% H ₂ O-	% total H ₂ O	% P ₂ O ₅
15	6.45	1.04			2.57	0.17
17	6.55	0.66	2.54	0.10	2.64	0.11
21	5.58	1.00	2.22	0.12	2.34	0.03
51	6.46	0.97			2.96	0.11
52	5.28	0.78	3.55	0.26	3.78	0.15
167	5.41	0.97	2.59	0.15	2.74	< 0.03
245	5.63	1.04			3.50	N.D.

* Analyst John Marinenko -- U. S. Geological Survey.



Table 6

Summation for allanite compositions

Wt. %	15	17	21	34	51	52	167	245
SiO ₂	30.0	29.5	30.4	28.0	29.8	30.6	30.8	30.4
Al ₂ O ₃	14.5	14.7	15.1	14.5	14.0	14.5	14.6	14.4
Fe ₂ O ₃	11.1	9.0	11.50	17.5	6.90	7.90	10.10	10.10
FeO	6.45	6.5	5.58		6.46	5.26	5.41	5.63
MgO	1.04	0.66	1.00	*	0.97	0.76	0.97	1.04
CaO	12.7	13.9	13.3	13.5	11.7	12.4	13.8	13.2
MnO	0.45	0.50	0.46	1.02	0.35	0.7	0.4	0.70
TiO ₂	0.92	0.56	0.77	0.86	1.05	0.88	0.60	0.87
P ₂ O ₅	0.17	0.11	0.03	*	0.11	0.15	<0.03	N.D.
CeO ₂	8.8	9.3	10.5	8.3	8.8	10.6	9.7	9.8
La ₂ O ₃	4.6	4.7	5.1	5.4	4.1	5.0	4.3	4.6
Nd ₂ O ₃	2.4	2.7	3.0	2.3	2.6	3.1	2.8	3.0
Sm ₂ O ₃	0.65	0.68	0.73	0.65	0.70	1.3	1.2	0.72
Gd ₂ O ₃	0.50	0.52	0.62	0.61	0.48	0.6	0.5	0.56
Y ₂ O ₃	< .1	< .1	< .1	0.20	< .1	< .1	< .1	0.20
ThO ₂	0.56	0.61	0.76	1.80	1.30	1.11	1.16	1.32
U ₃ O ₈	0.01	0.01	0.01	*	0.02	0.02	0.02	0.01
H ₂ O-		0.10	0.12	*		0.26	0.15	
H ₂ O+	2.37				2.96		3.55	3.50
Total	97.22	96.59	101.00	94.44	92.28	98.93	99.10	100.05

* Not determined.

N. D. Not detected.

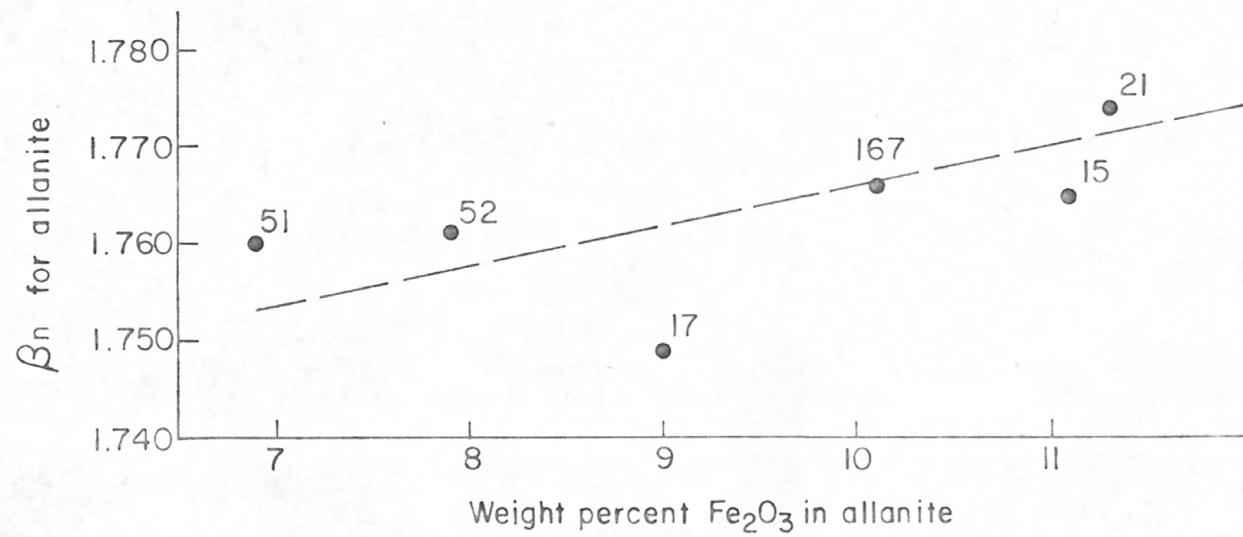


Figure 1 Plot of beta index for allanite against Fe_2O_3 content of allanite.

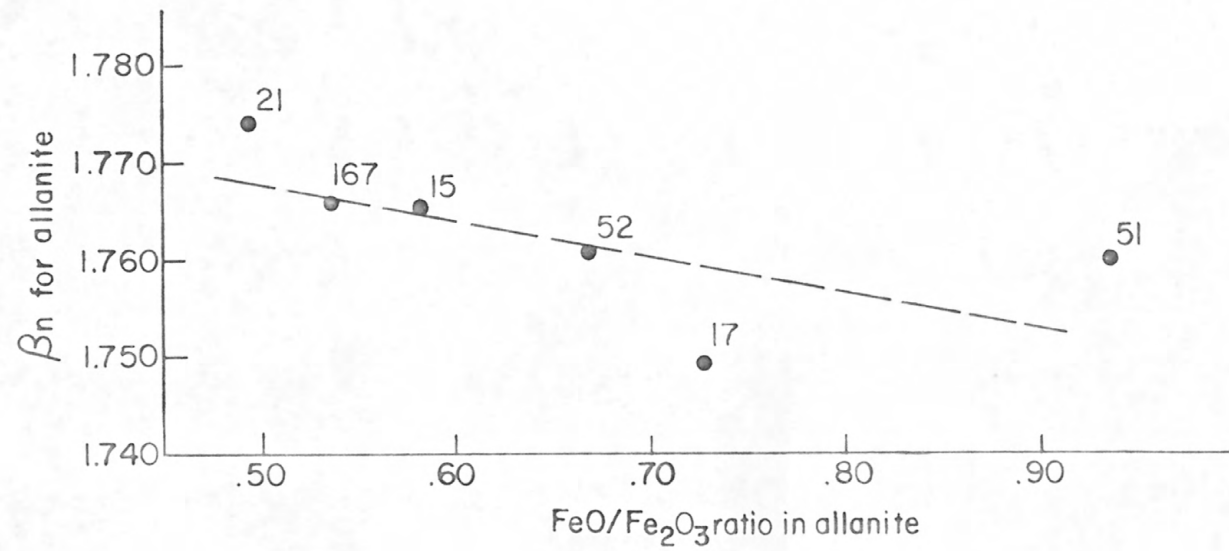


Figure 2 Plot of beta index for allanite against $\text{FeO}/\text{Fe}_2\text{O}_3$ ratio for allanite.

points results, indicating that the increase in indices of refraction is a function of Fe_2O_3 content rather than of total iron as Figures 1 and 2 illustrate. This relationship between refractive indices and Fe_2O_3 content is supported by a study of ^{8/} allanite from Yosemite National Park by Hutton, 1951.

It is also thought that increasing rare earth content in allanite will result in higher refractive indices, but proof has generally been lacking due to the incompleteness of optical data on allanites from a single series of differentiated and, therefore, related rocks. Most optics given for allanite in the literature are for pegmatitic allanites from hundreds of widely separated localities. Plots of β_n against weight percents of the three most abundant rare earth oxides (CeO_2 , La_2O_3 , Nd_2O_3) in the allanites from the Boulder Creek batholith are shown in Figures 3, 4, and 5. The plot of β_n against CeO_2 (Figure 3), the most abundant rare earth oxide, shows a definite field of increase with increasing CeO_2 with a large scatter of the points. Figure 4 shows a complete scatter of points when β_n is plotted against La_2O_3 , the second most abundant of the rare earth oxides. However, when β_n is plotted against Nd_2O_3 , Figure 5, which accounts for only 2-3% by weight of the bulk composition, the same trend is shown as in the plot against CeO_2 except the horizontal scale is shorter. Figure 6, which is a plot of the sum of those constituent oxides which tend to increase the

^{8/} Hutton, C. O., 1951, "Allanite from Yosemite National Park, Tuolumne County, California", American Mineralogist, vol. 36, nos. 3 and 4, pp. 233-247.

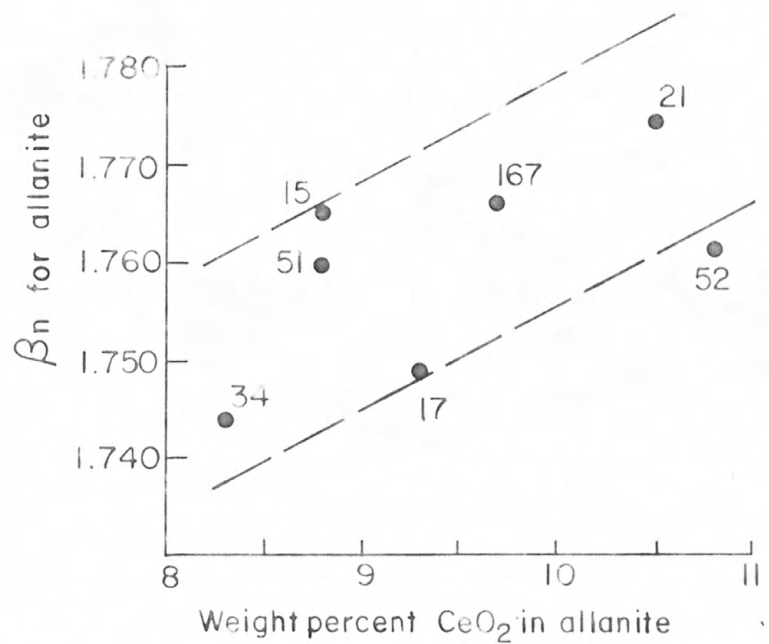


Figure 3 Plot of beta index for allanite
against CeO_2 content of allanite.

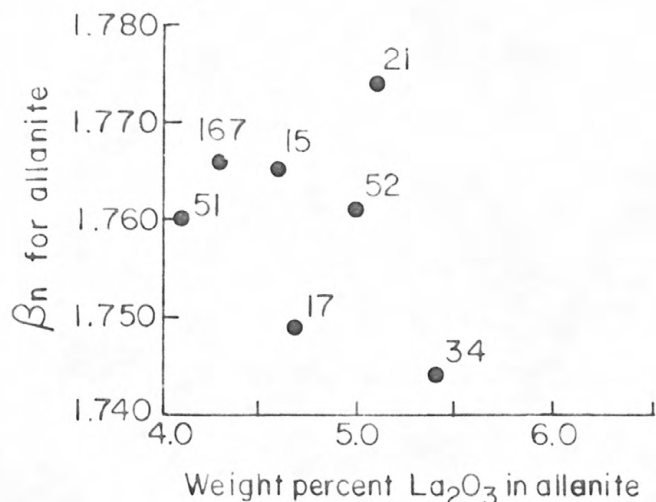


Figure 4 Plot of beta index for allanite
against La_2O_3 content of allanite.

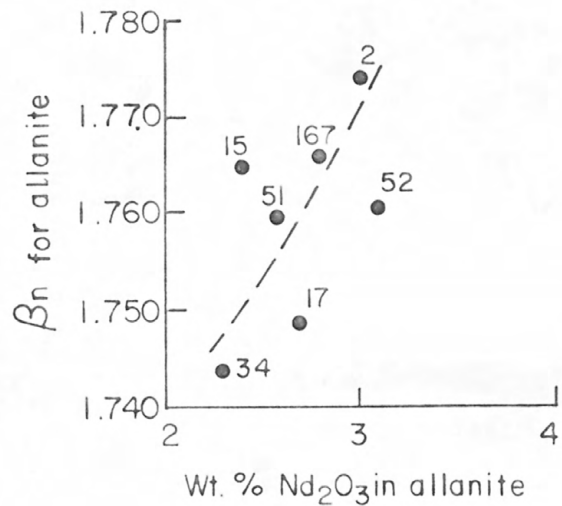


Figure 5 Plot of beta index for allanite against Nd_2O_3 content of allanite.

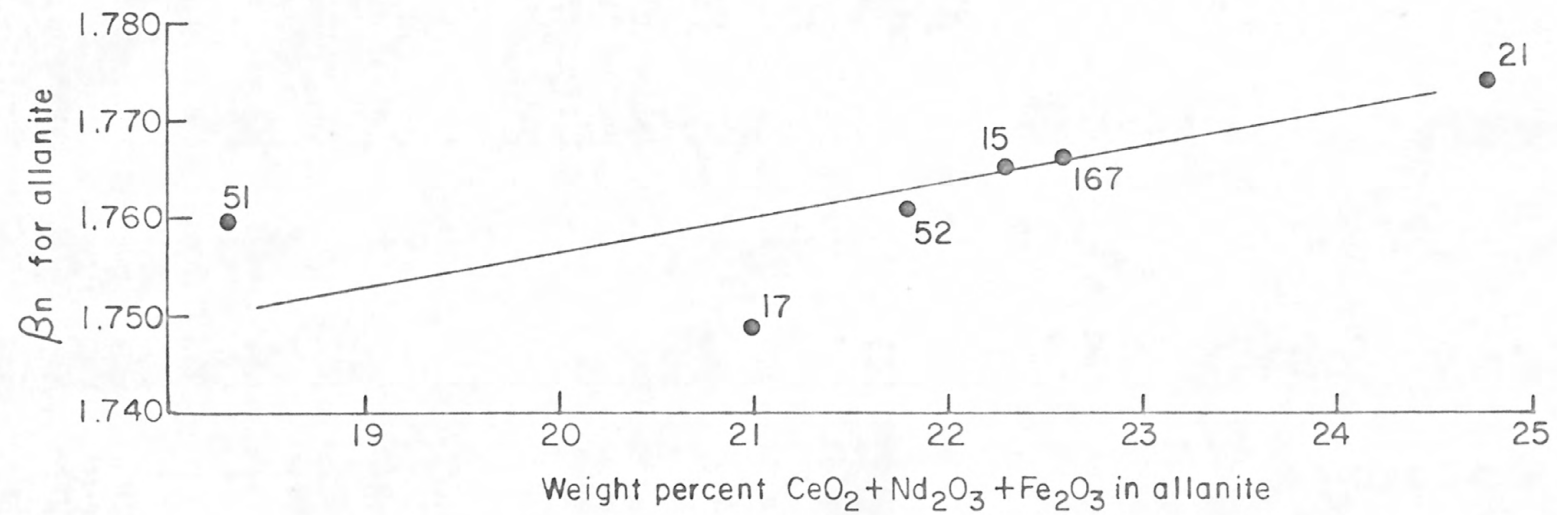


Figure 6 Plot of beta index for allanite against the sum $\text{CeO}_2 + \text{Nd}_2\text{O}_3 + \text{Fe}_2\text{O}_3$ in allanite.

refractive indices (CeO_2 , Nd_2O_3 and Fe_2O_3) against SiO_2 , shows the same trend as the three separate plots but with a marked decrease in scatter of points. The trend shown in Figure 6 supports the conclusion that the increase in refractive indices for the suite of allanites studied is related to the increase of at least some of the rare earths as well as to Fe_2O_3 content.

Figures 7, 8, and 9 show plots of the three major rare earth oxides for these allanites (CeO_2 , La_2O_3 , and Nd_2O_3) as weight percent of bulk composition of the allanites against the weight percent of SiO_2 for the bulk rock composition. Figure 7 shows a good trend of increasing CeO_2 with increasing SiO_2 , but samples 15 and 51 fall below. It will be noted in Table 6 that the chemical composition summation is much lower for 51 than it is for the others. It is possible this low summation is due in part to low values for some of the rare earths but this has not been established. Sample 15 belongs to a group of rocks on which low apparent ages were obtained using the $\text{Pb}-\alpha$ method on zircons from 9/ those rocks. This group of rocks will be discussed later in the text. Figure 8 shows the same increase of La_2O_3 with increasing SiO_2 with 51 again falling below the main trend. Figure 9 shows the increase of Nd_2O_3 with SiO_2 with 15 again falling below the trend. The plot of total rare earth oxides, including the lesser quantities of Sm_2O_3 and Gd_2O_3 , against SiO_2 from the bulk rock is shown in Figure 10. Samples 15 and 51, as might be surmised from the preceding plots, fall well below the main trend of increasing

9/ Phair, C., and Gottfried, D., unpublished data.

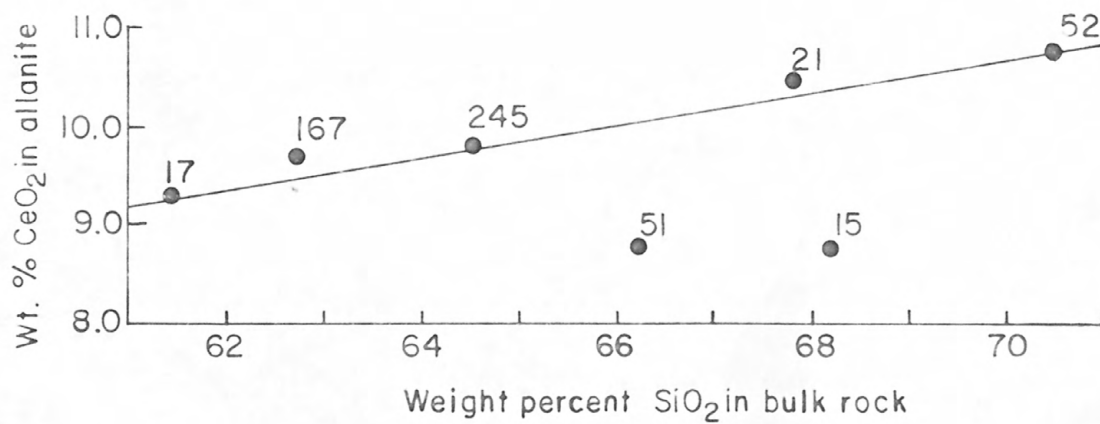


Figure 7 Plot of CeO_2 content of allanite against the SiO_2 content of bulk rock.

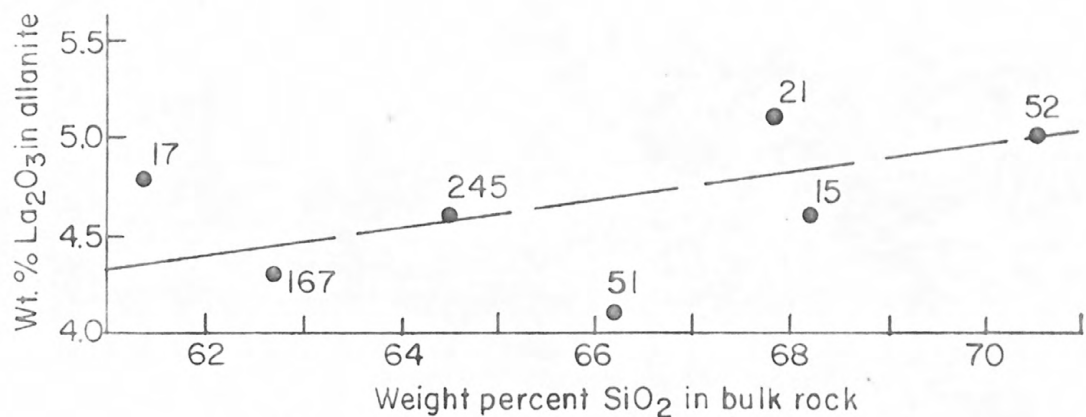


Figure 8 Plot of La_2O_3 content of allanite against SiO_2 content for bulk rock.

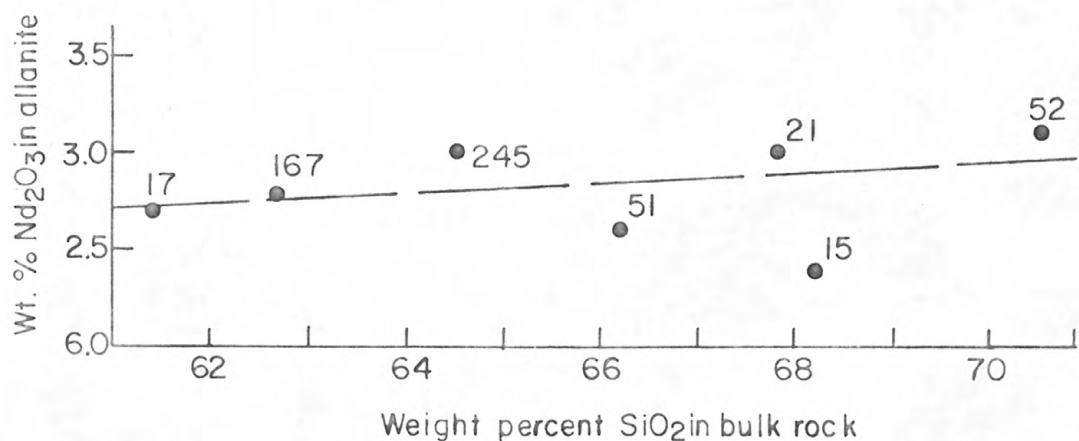


Figure 9 Plot of Nd_2O_3 content of allanite against SiO_2 content for bulk rock.

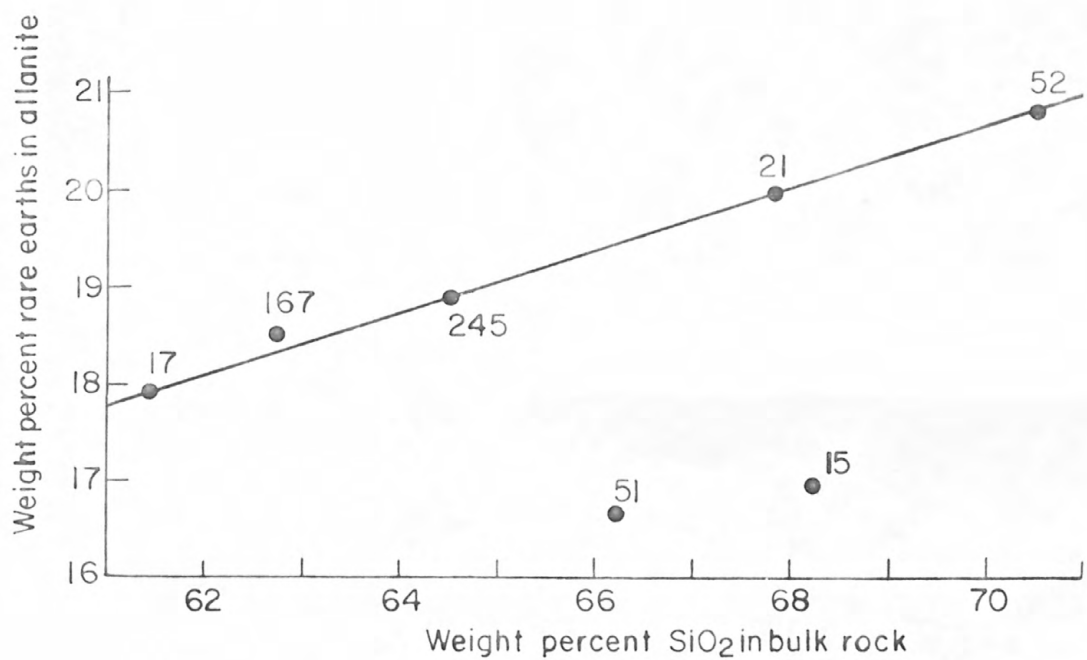


Figure 10 Total rare-earth oxide content of allanite plotted against SiO_2 content for bulk rock.

rare earths in allanite with increasing SiO_2 from the bulk rock. Figure 11 shows the distribution of the individual rare earth oxides recalculated to 100% of total rare earth oxides for these allanites plotted according to rock type. It should be noted that only three samples represent granodiorite, three samples represent quartz monzonite and two samples represent granite. As can be seen from Figure 11, CeO_2 equals about 50% total rare earths, La_2O_3 about 25%, Nd_2O_3 about 15%, and Sm_2O_3 and Gd_2O_3 about 5% and 3% respectively of total rare earths in these allanites. The total rare earth contents are highest in allanite from granites as expected from preceding plots (Figures 7, 8, 9, and 10) of rare earths against SiO_2 for the bulk rock, but the allanites from the granodiorites show a higher content of total rare earths than those allanites from the quartz monzonites which is not expected. It is pointed out, however, that of the three samples representing quartz monzonite, two of them are samples 15 and 51 whose anomalous characteristics have already been pointed out. The writer believes that analyses for other perhaps more representative quartz monzonites would probably show a rare earth content for their allanites higher than that for the allanites from the granodiorites.

Metamictization

It was felt that this suite of allanites would be particularly well suited to a study of the problem of metamictization. Although unusually fresh, highly birefringent for allanites, there is a range of birefringence within this suite as determined by optical measurements of α and γ indices.

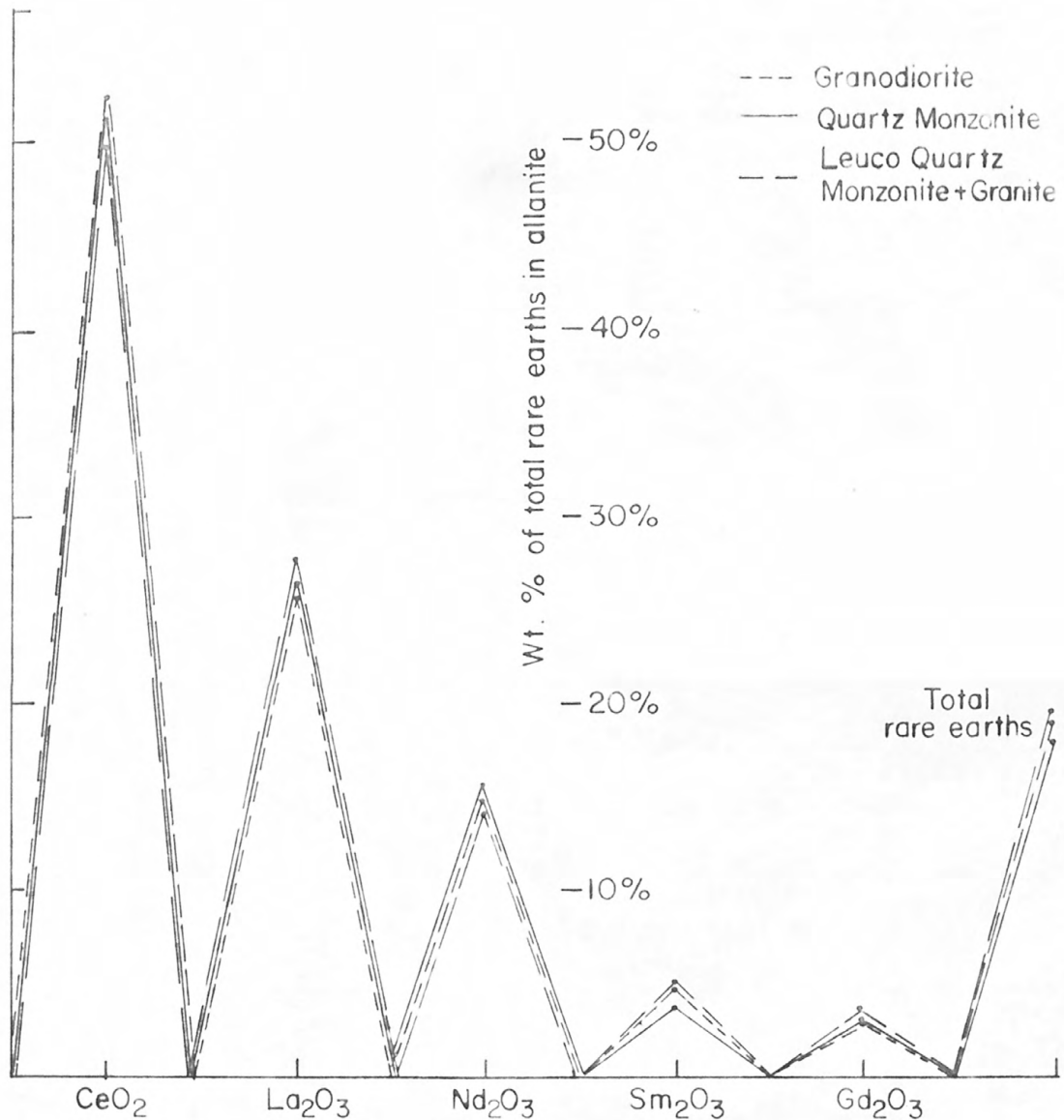


Figure II Combined plot showing individual rare-earth oxides from allanite recalculated to 100% and plotted as to rock type.

Birefringence may be stated numerically as $\frac{N_y - N_x}{N_y + N_x}$ and in these samples it ranges from 0.020 to 0.032.

The process of metamictization involves the gradual destruction of the internal crystal structure as a result of the bombardment from within of the crystal lattice by the alpha particles emitted by the contained radioactive elements and the accompanying recoil of the emitting nuclei. Previous workers have postulated several probable mechanisms of this process of converting a crystalline substance into a non-crystalline substance; of these the mechanism proposed by Holland and Gottfried ^{10/} seems to be the best documented.

Progressive alteration of whatever origin often changes the optics of a crystalline substance. Available data on allanite show that those supposed metamict varieties have very low birefringence or are isotropic and those least metamict have higher birefringence. The degree of alteration of these allanites therefore can be estimated on the basis of variations in birefringence.

No definite trend was discernable relating birefringence to water content. However, plots of uranium and thorium versus

^{10/} Hurley, P. M., and Fairbairn, H. W., 1953, "Radiation Damage in Zircon: a possible age method", Bull. Geol. Soc. Am., vol. 64, p. 659; Slater, J. C., 1951, "Effects of Radiation on Materials", Jour. Appl. Phys., vol. 22, p. 237; Ueda, T., and Korekawa, M., 1954, "On the Metamictization", Memoirs of the College of Science, University of Kyoto, Series B, vol. XXI, no. 2, Japan.

^{11/} Holland, H. D., and Gottfried, D., 1955, "The Effect of Nuclear Radiation on the Structure of Zircon", Acta Crystallographica, vol. 8, Pt. 6, pp. 291-300.

birefringence clearly show that birefringence decreases with increasing content of uranium and thorium. Figure 12 shows increasing ThO_2 values following the lower values for birefringence. The alpha particle emission for a given amount of uranium is about four times that of an equal amount of thorium, so Figure 13 shows birefringence plotted against $U + \frac{1}{2} \text{Th}$ in parts per thousand to better balance the alpha emission of the two radioactive elements. The same trend is observed as in Figure 12 but with a slightly greater scatter of points. This shows the major role that thorium plays in the alteration of these allanites and also confirms that this is alteration resulting from the process of metamictization.

A decrease in birefringence should show a corresponding decrease in refractive indices. This is shown in Figure 14 where β_n is plotted against birefringence. A major trend of β_n increasing with increasing birefringence is shown with some scatter of points, but in addition there also appears to be a smaller sub-parallel trend off set towards the higher indices and lower birefringence portion of the coordinates. On Plate 1 it is seen that samples 21, 50, 51, 53, and 84, comprising this secondary trend on Figure 14, form a north-south alignment near the southwestern border of the Boulder Creek batholith. Further petrologic study is needed to disclose whether a real belt does exist there, or if it is fortuitous, and if this "belt" has been subjected to some "thermal event" for some reason restricted to that particular portion of the batholith.

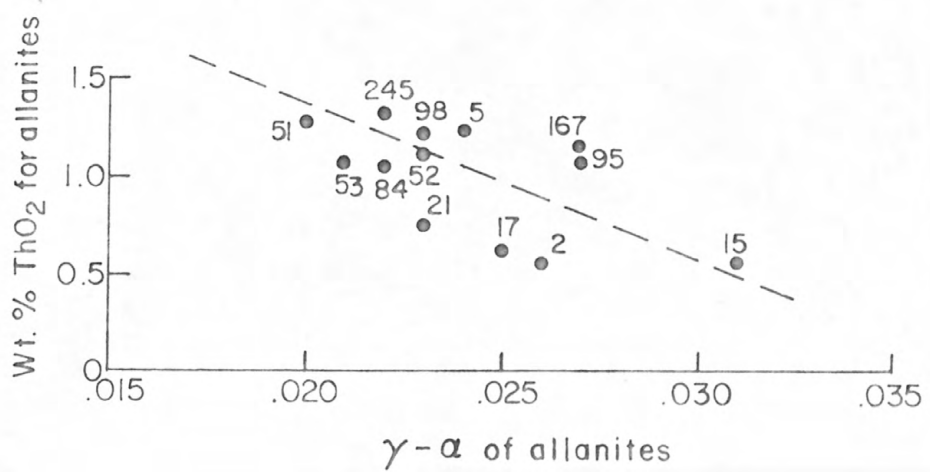


Figure 12 Th_{O₂} content of allanite plotted against birefringence of allanite.

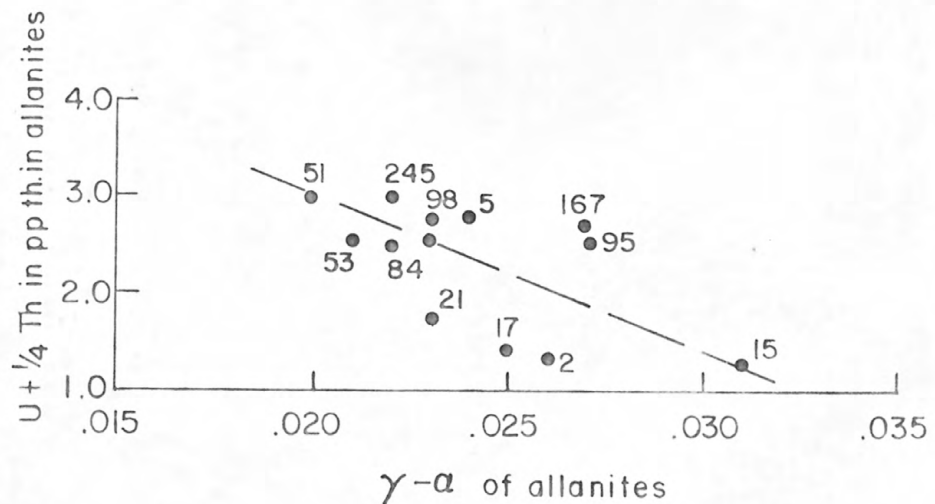


Figure 13 U + $\frac{1}{4}$ Th content of allanites in parts per thousand plotted against birefringence of allanite.

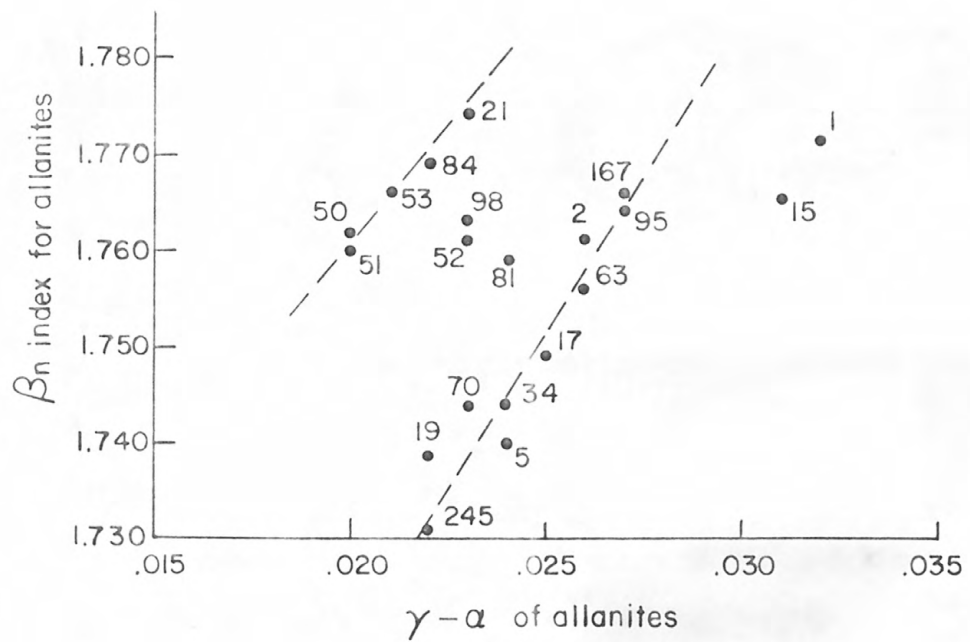


Figure 14 Beta index for allanite plotted against birefringence of allanite.

12/

It has been noted by Holland and Gottfried (1955) that during the metamictization of zircon the extraordinary direction of index (the highest index) is effected more readily than the ordinary direction (direction of lowest index). It was decided to see if the larger index (γ) was affected more readily than the smallest index (α) for these allanites. Figure 15 is a combined plot of α , β , and γ indices against an expanded scale for birefringence for these allanites. The figure shows that within both the major trend and the minor trend pointed out in Figure 14, the β and γ indices increase at the same rate with respect to birefringence and the α indices increase at a slightly smaller rate. It is shown then that with increasing metamictization the decrease in β and γ indices is more rapid than the decrease in α indices in these allanites.

The problem of low apparent age [REDACTED] rocks in the midst of over all higher age [REDACTED] rocks, which structurally seem to be contemporaneous, was recognized in the 15/ zircon study by Phair and Gottfried of this batholith. As in that zircon study, plots of uranium and thorium content of these allanites against SiO_2 content for the bulk rock and the lime-alkali ratio ($\frac{\text{CaO}}{\text{Na}_2\text{O} + \text{K}_2\text{O}}$) for bulk rock composition show two general groupings of samples. The group lowest in uranium and thorium content is in all cases where age data (Pb-alpha on zircon) is available, comprised of rocks whose zircons gave

12/ Holland, H. D., and Gottfried, D., 1955, op. cit.

13/ Phair, G., and Gottfried, D., unpublished data.

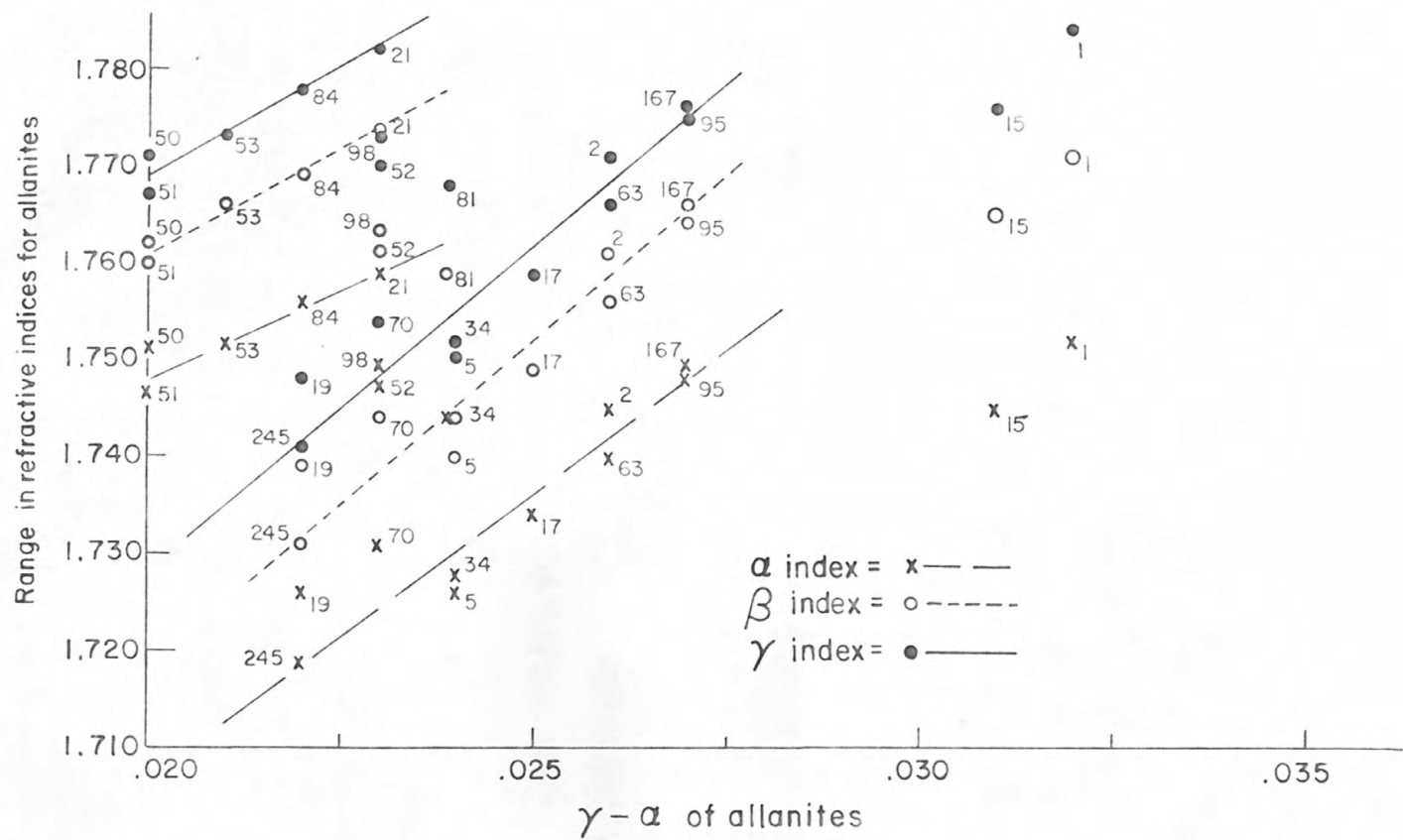


Figure 15 Combined plots of alpha, beta and gamma indices for allanite against an expanded scale of birefringence for allanite.

apparent low ages. Figure 16 shows the uranium content of the allanites plotted against weight percent SiO_2 for the bulk rock. Two general fields are seen. The upper field consists of the higher age rocks with no particular correlation to increasing SiO_2 . The lower group consists of 2, 5, 15, 17, 21, and 245. Pb-alpha ages are not available for 5 and 245, but the other four samples are low-age rocks. Figure 17 is a plot of ThO_2 of these allanites against SiO_2 in the bulk rock. Two general fields are seen again with the lower group again being 2, 15, 17, and 21. Figure 18 a plot of thorium against the lime/alkali ratio for the bulk rock, shows as the lower scatter of points 2, 15, 17, and 21, all low-age rocks. Figure 19 is a plot of thorium against the Th/U ratio and Figure 20 is uranium plotted against the Th/U ratio for these allanites. In both cases the low-age group falls away from the main group. Phair and Gottfried (oral communication) feel that quite possibly these rocks of apparent low age may have had some thorium, uranium and radiogenic lead leached while undergoing later deformation. This writer has grouped these rocks according to extent or degree of foliation and found that samples 2, 15, 17, and 21 are all within the top third group of most foliated rocks. This is compatible with the hypothesis that the more deformed (foliated) rocks may have lost a portion of their uranium, thorium, and radiogenic lead during deformation possibly due to leaching of the elements by hydrothermal fluids of low pH.

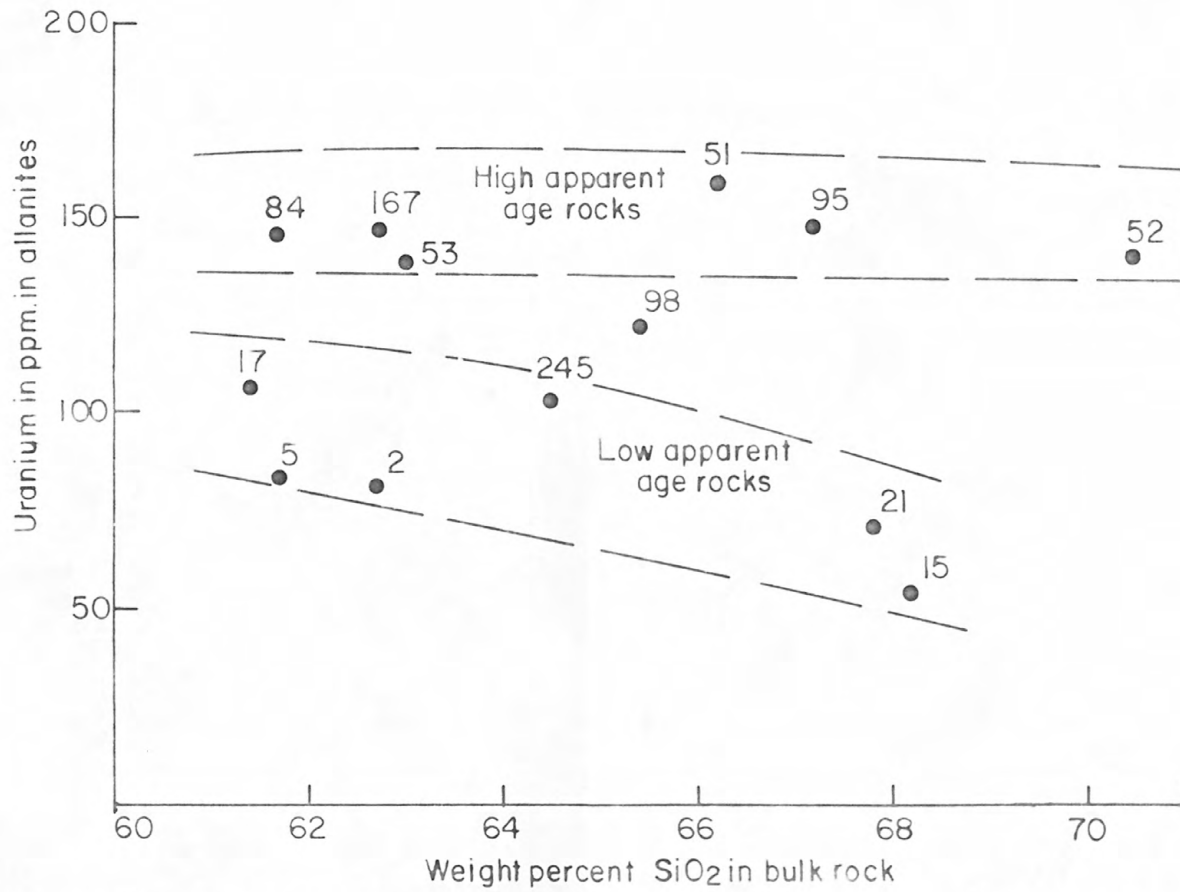


Figure 16 U content of allanites plotted against SiO_2 content for bulk rock.

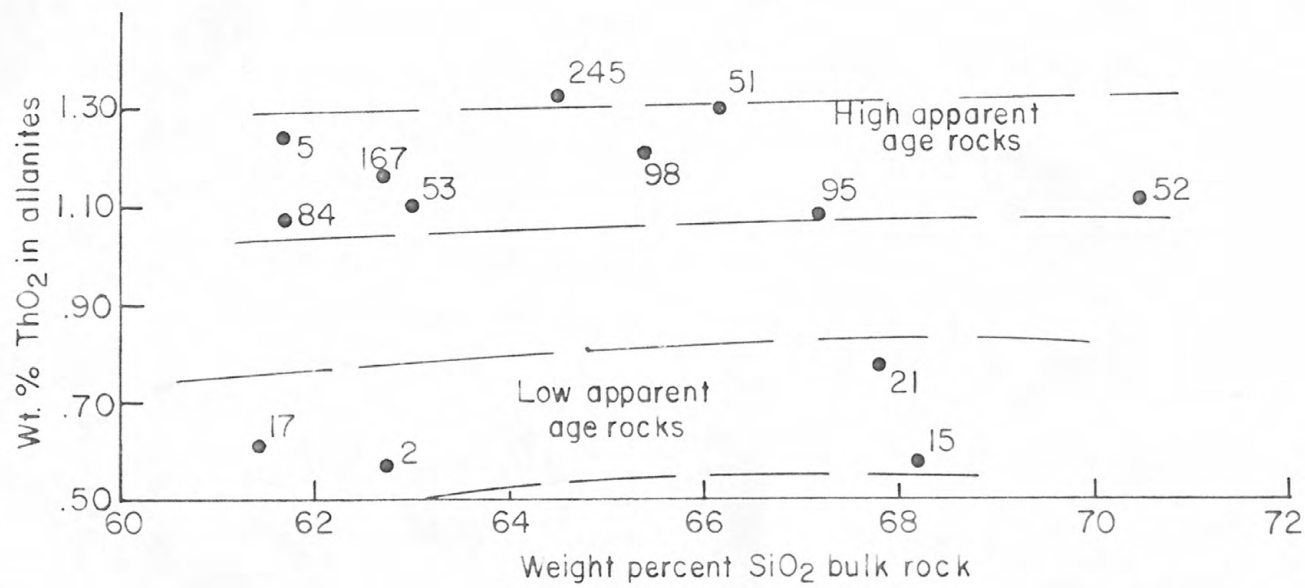


Figure 17. ThO_2 content of allanites plotted against SiO_2 content for bulk rock.

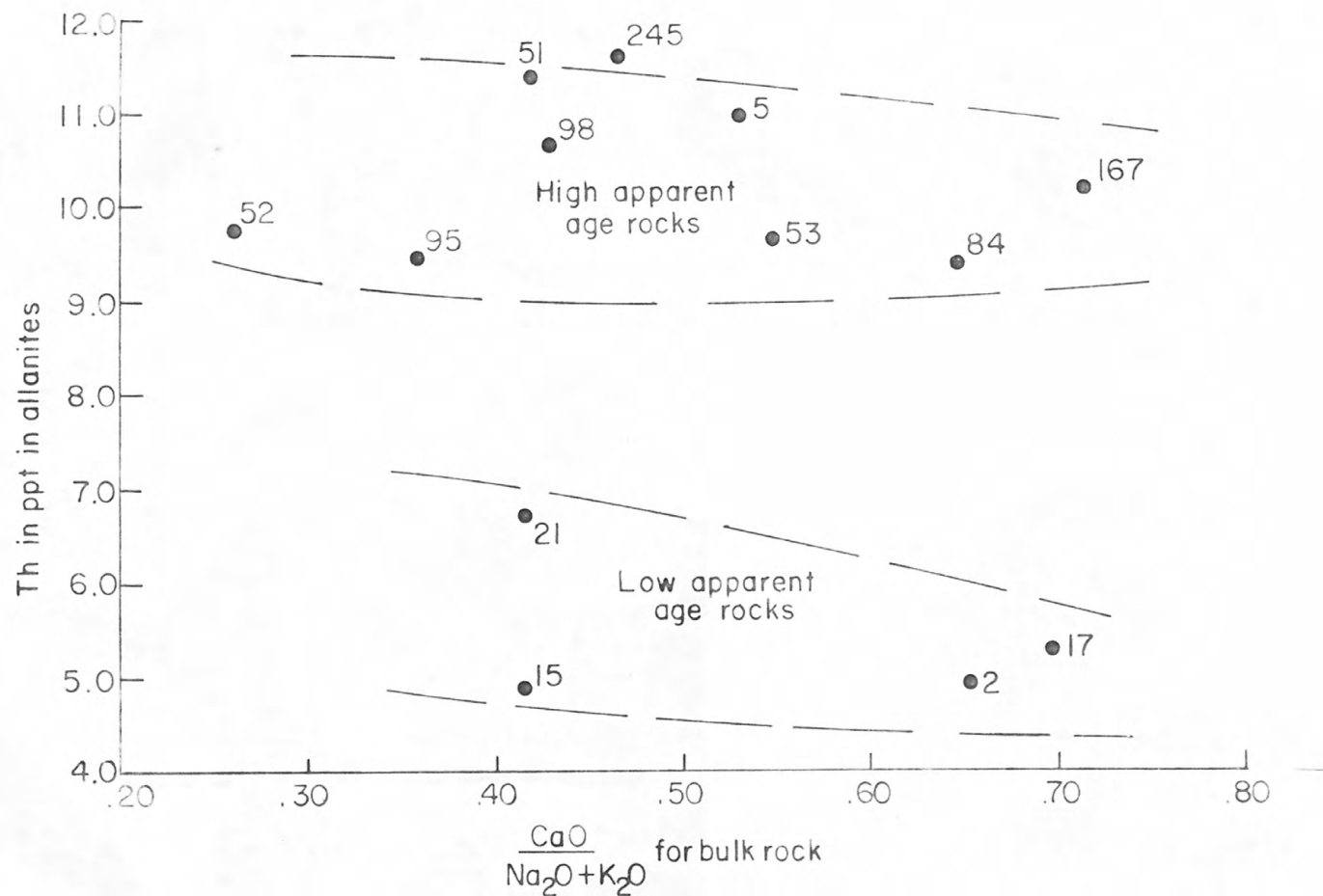


Figure 18 Plot of Th content of allanite in parts per thousand against the lime-alkali ratio of bulk rock.

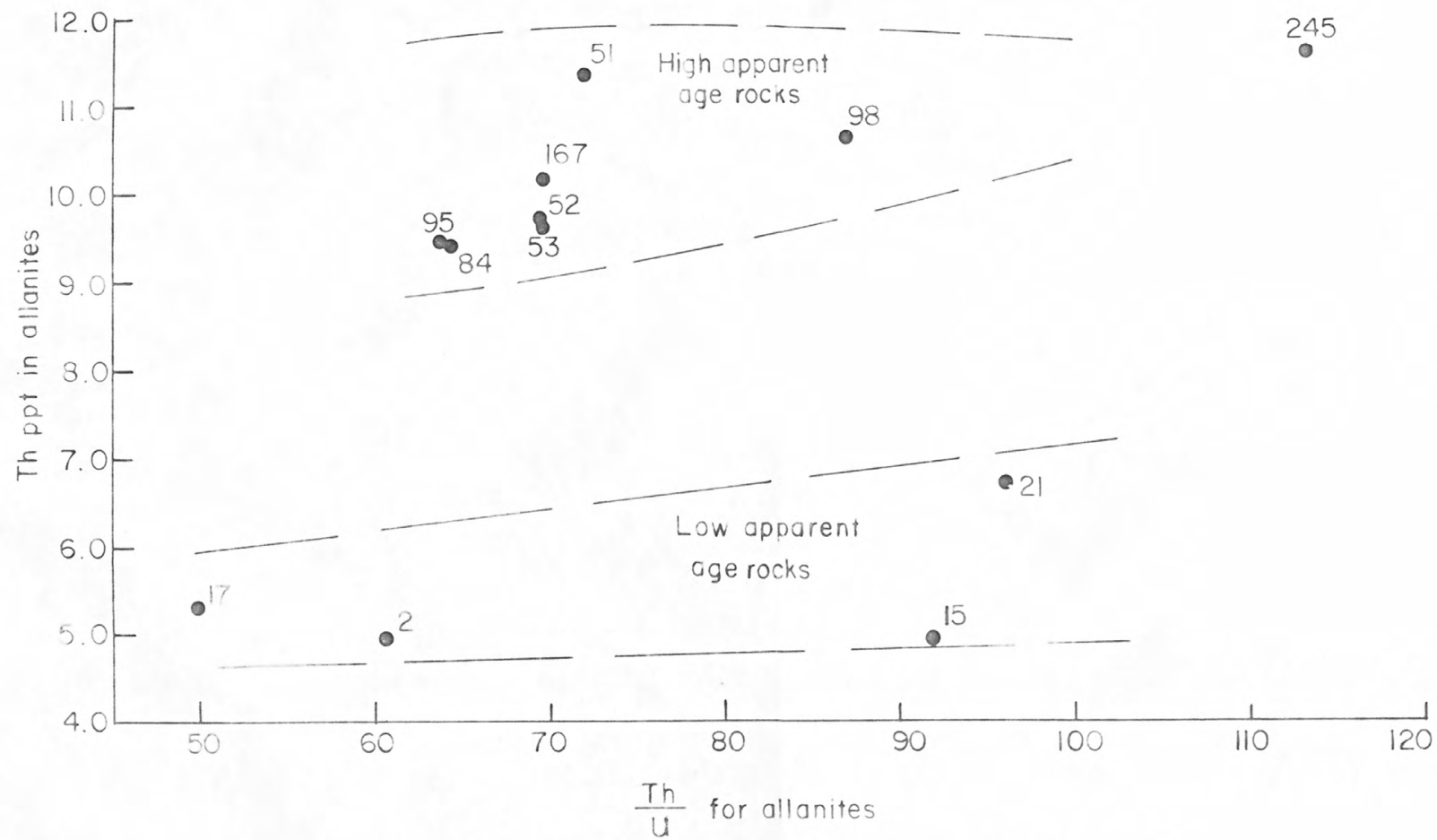


Figure 19 Plot of Th content of allanite against the Th/U ratio for allanite.

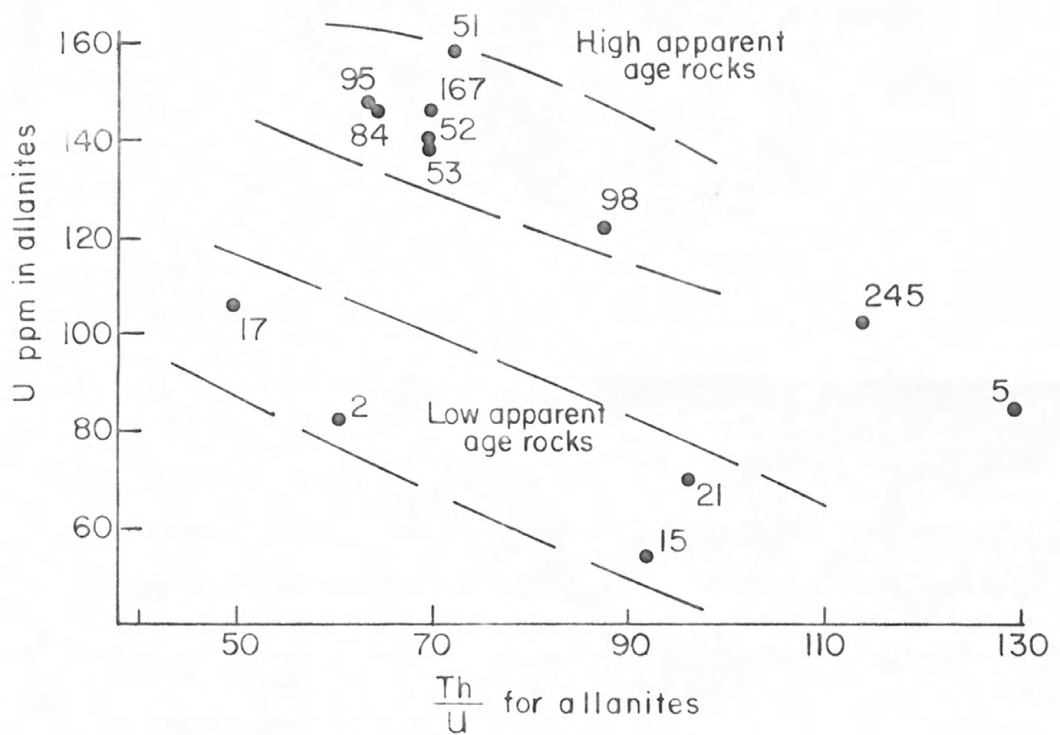


Figure 20 Plot of U content of allanites against Th/U ratio for allanite.

From observation of allanite in hand specimen and in thin section, it has been observed that the long axis of the allanite shows no preferred direction of orientation with respect to the foliation. Allanite is normally found in the felsic bands of these foliated rocks but always associated with clots of mafic minerals. Biotite was always present in these mafic clots with the other mafics consisting of hornblende and opaque accessories. Plate 2 shows several drawings of allanite and its associated minerals as seen in thin section with a petrographic microscope. Epidote in all cases at least partially rims the allanite, and, in many cases, the allanite is a relatively small core within euhedral epidote. The drawings illustrate that when incomplete epidote rimming of the allanite occurs the epidote has formed only along those regions of the allanite in contact with biotite and is absent where in contact with quartz, plagioclase and microcline. It was also noted that the smaller the allanite cores relative to the thickness of the epidote rim, the less euhedral is the crystal habit of the allanite. The larger the allanite core with respect to the epidote rim the more prismatic is the allanite.

The allanite formed after the rocks were foliated and is probably of deuterio origin. Lovering and Goddard believe the rocks were at least partially foliated during emplacement after most of the major rock-forming minerals had crystallized. The

^{14/} Lovering, T., and Goddard, E. N., 1950, op. cit.

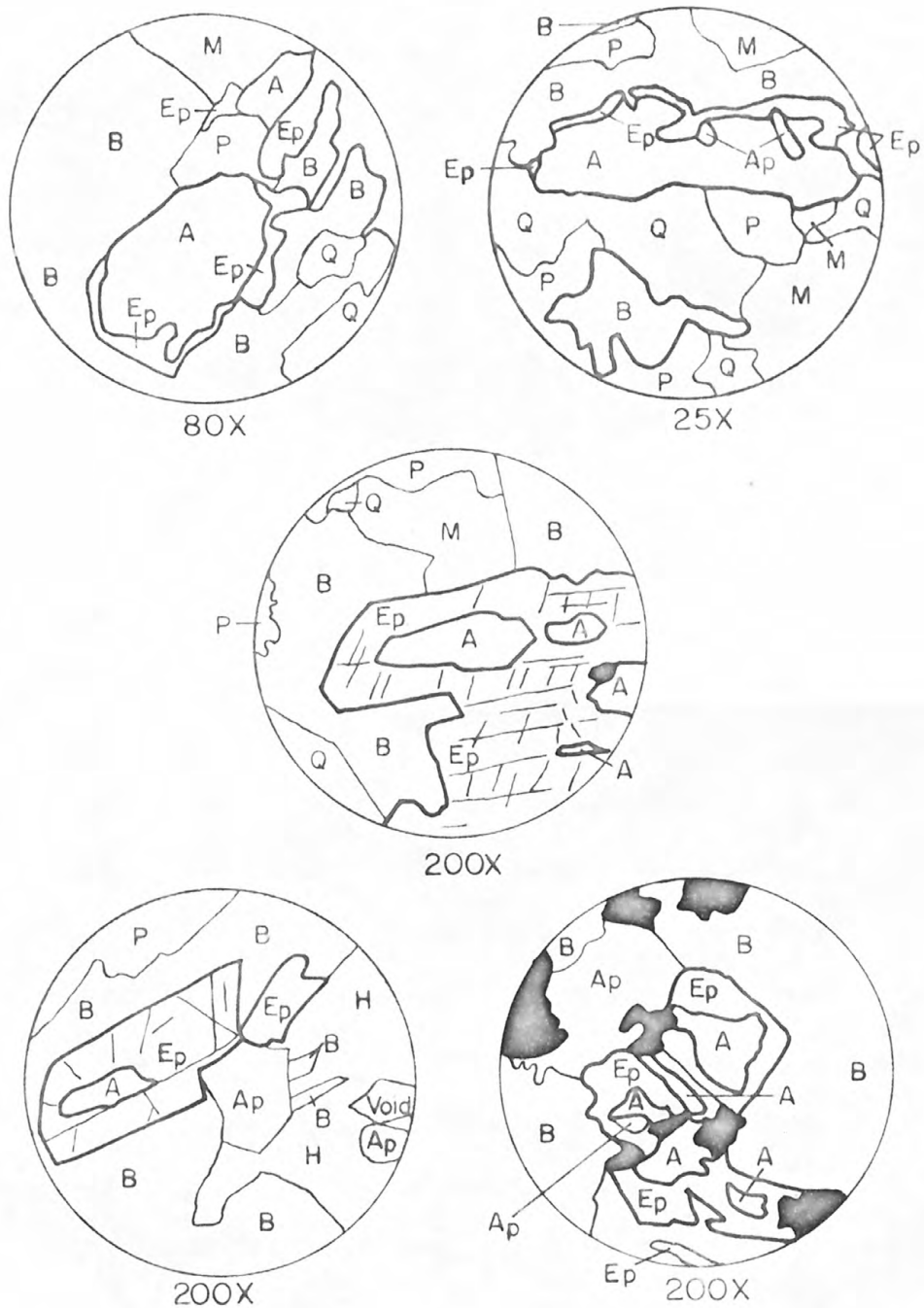


Plate 2 Sketches of allanite and epidote and their associated minerals as observed in thin section.

A	allanite
Ap	apatite
B	biotite
Ep	epidote
M	microcline
P	plagioclase
Q	quartz

generally uniform chemical composition of these allanites also suggests a deuteritic origin as they probably crystallized from a residual fluid of relatively homogeneous composition that pervaded the entire batholith. These factors indicate the age for these allanites as probable late Precambrian. Because of the epidote-rimming relations the epidote is considered to be later than the allanite, in fact, it may be as late as the Laramide orogeny. ^{15/} Lovering and Goddard, 1950, have pointed out the common occurrence of hydrothermal epidote in the tungsten veins of the Laramide mineral belt. Many of these tungsten veins cut across the northwestern part of the Boulder Creek batholith.

There is some data available on allanites from granitoid rocks. ^{16/} Lee and Bastron, 1962, describe allanite from a quartz monzonite intrusive of Jurassic(?) age having a slightly higher range of refractive index and birefringence than those from the Boulder Creek batholith but having nearly equal amounts of rare-earth and ThO_2 content as the allanites studied here.

^{17/} Smith, et. al., 1957, report allanites from granodiorites, quartz monzonite and granites of Late Jurassic or Cretaceous age with refractive indices and birefringence slightly lower than for those reported here on the allanites from the Boulder Creek

15/ Lovering, T., and Goddard, E. N., 1950, op. cit.

16/ Lee, D. E., and Bastron, H., 1962, "Allanite From the Mt. Wheeler Area, White Pine County, Nevada", American Mineralogist, vol. 47, nos. 11 and 12, pp. 1327-1331.

17/ Smith, W. L., Franck, M. L., and Sherwood, A. M., 1957, "Uranium and Thorium in the Accessory Allanite of Igneous Rocks", American Mineralogist, vol. 42, nos. 5 and 6, pp. 567-577.

batholith but with nearly the same range in rare-earth and ThO_2 content as those from the Boulder Creek batholith. A heating affect may have restored the crystallinity of the allanites studies here some time since the Precambrian, for if they are truly that old it might be expected they should be more metamict than they are.

Summary and Conclusions

Several principal conclusions may be drawn from this detailed study of allanites from rocks of the Boulder Creek batholith:

1. The refractive indices of the suite of allanites studied increase with increasing Fe_2O_3 , CeO_2 , and Nd_2O_3 content. ^{18/} Hasegawa, 1960, who has probably contributed more information to the literature on the compositions of allanites than any other researcher, could not detect any distinct relations between optics and composition. This is probably directly related to the fact that he was dealing with pegmatitic allanites from a large number of localities representing diverse geochemical environments. The observations of the relationship between optics and composition of the allanites in this paper were no doubt facilitated by a common geochemical environment for the host rocks.

^{18/} Hasegawa, S., 1960, "Chemical Compositions of Allanite", The Science Reports of the Tohoku University, Series III, vol. VI, no. 3, pp. 331-387, Japan.

2. The total rare-earth content of these allanites increases slightly with increasing silica for the bulk rock. Average percentages of the rare-earth oxides recalculated to percent of total rare-earths show that Ce_2O_3 constitute about 50%; La_2O_3 25%; Nd_2O_3 15%; Sm_2O_3 5%; and Gd_2O_3 about 3%. These percentages of rare-earths vary by only a few percent for allanites separated from granodiorite, quartz monzonite and granite of the Boulder Creek batholith.

3. The uranium and thorium content show no apparent correlation to either lime-alkali ratio or silica content for the bulk rock, but it is of interest to note that the allanites with low uranium and thorium content comprise a group which give low apparent ages determined by the Pb-alpha method on zircons from those rocks; and the uranium and thorium content of those zircons was also lower than for the zircons of higher apparent age rocks. This correlation of relatively low uranium and thorium content in allanite and zircon with low apparent age rocks and the usually higher degree of foliation of those same rocks lends support to the hypothesis of Phair and Gottfried that these radioactive elements and radiogenic lead have in some way been partially leached from the rocks, possibly during later deformation.

4. Those allanites of this suite with the highest uranium and thorium content are the most metamict and those with lower amounts of uranium and thorium are least metamict. Radioactive decay of thorium is the dominant process in the metamictization of these allanites as it is one hundred times as abundant than the uranium. It was also found that in allanites such as these from the Boulder Creek batholith, which are fresh enough for

precise refractive indices determination, that optical methods appear to be a more sensitive indicator of the degree of metamictization than variations in X-ray d-spacings. The decrease in β and γ index during metamictization is more pronounced than the decrease in α index.

5. Allanite in the Boulder Creek batholith is probably a late-stage deuteritic mineral formed after the main rock-forming minerals had crystallized and after the rocks were foliated. From textural evidence, epidote appears to be later than the allanite; the epidote may be a hydrothermal product associated with the Laramide metallization.

6. The allanite is unusually fresh considering its age (■ Precambrian) and its content of radioactive elements which is comparable to the content of many metamict varieties from other localities. Perhaps the geothermal regime associated with the Laramide orogeny and the length of time of that orogeny may have been sufficient to restore some of the allanite structure.

In summary, this study, aside from increasing our knowledge of the mineralogy and chemistry of the allanite group in general, provides additional data on the partitioning of rare-earths in a consolidating magma and on the role of decay of radioactive elements in metamictization. These data, together with other corroborative petrologic and geologic observations, furnish another, heretofore overlooked tool in reconstructing the geologic history of batholithic rocks.

Acknowledgements

The writer would like to thank Professor M. F. Norton for his interest and helpful suggestions throughout this investigation. Special thanks are extended my colleagues of the U. S. Geological Survey: to Harry Rose, Robena Brown, Roosevelt Moore, and John Marinenko for supplying the chemical data; to George Phair and David Gottfried for making available to me much of their unpublished data and opinions formulated during several years of petrologic study of the Boulder Creek batholith; and to Robert Tilling for his informal but thoughtful review of the manuscript.

Bibliography

Davis, G. L., Aldrich, L. T., Tilton, G. R., Wetherill, G. W., and Jeffery, P. M., 1956, "The Age of Rocks and Minerals", Annual Report of the Director of the Geophysical Laboratory, Carnegie Institution of Washington, No. 1265, p. 165.

—, Tilton, G. R., Aldrich, L. T., Wetherill, G. W. and Faul, H., 1957, "The Age of Rocks and Minerals", Annual Report of the Director of the Geophysical Laboratory, Carnegie Institution of Washington, No. 1277, p. 166.

Deer, W. A., Howie, R. A., and Zussman, J., 1962, Rock Forming Minerals. New York: John Wiley and Sons, Inc., vol. 1, p. 211.

Hasegawa, S., 1960, "Chemical Compositions of Allanite", Science Reports of the Tohoku University, Series III, vol. VI, no. 3, pp. 351-387, Japan.

Holland, H. D., and Gottfried, D., 1955, "The Effect of Nuclear Radiation on the Structure of Zircon", Acta Crystallographica, vol. 8, Pt. 6, pp. 291-300.

Murley, P. M., and Fairbairn, H. W., 1953, "Radiation Damage in Zircon: a possible age method", Bull. Geol. Soc. Am., vol. 64, p. 659.

Hutton, C. O., 1951, "Allanite from Yosemite National Park, Tuolumne County, California", American Mineralogist, vol. 36, nos. 3 and 4, pp. 233-247.

Lovering, T. S., and Goddard, E. N., 1950, "Geology and Ore Deposits of the Front Range Colorado", U. S. Geological Survey Professional Paper 223, 319 pp.

Lee, D. E., and Bastron, H., 1962, "Allanite From the Mt. Wheeler Area, White Pine County, Nevada", American Mineralogist, vol. 47, nos. 11 and 12, pp. 1327-1331.

Phair, G., and Fisher, F. G., 1962, "Laramide Conamgnetic Series in the Colorado Front Range: The Feldspars", Petrologic Studies: A Volume to Honor A. F. Buddington, Geol. Soc. Am., pp. 479-522.

Slater, J. C., 1951, "Effects of Radiation on Materials", Jour. Appl. Phys., vol. 22, p. 237.

Smith, W. L., Franck, M. L., and Sherwood, A. M., 1957, "Uranium and Thorium in the Accessory Allanite of Igneous Rocks", American Mineralogist, vol. 42, nos. 5 and 6, pp. 367-377.

Ueda, T., and Korekawa, M., 1954, "On the Metamictization",
Memoirs of the College of Science, University of Kyoto,
Series B, vol. XXI, no. 2, Japan.

Wilcox, R. E., 1959, "Use of Spindle Stage For Determining
Refractive Indices of Crystal Fragments", American
Mineralogist, vol. 44, pp. 1272-1293.

Ueda, T., and Korekawa, M., 1954, "On the Metamictization",
Memoirs of the College of Science, University of Kyoto,
Series B, vol. XXI, no. 2, Japan.

Wilcox, R. E., 1959, "Use of Spindle Stage For Determining
Refractive Indices of Crystal Fragments", American
Mineralogist, vol. 44, pp. 1272-1293.

PAMPHLET BINDERS

This is No. 1933

also carried in stock in the following sizes

	HIGH	WIDE	THICKNESS		HIGH	WIDE	THICKNESS
1523	9 inches	7 inches	$\frac{1}{2}$ inch	1523	12 inches	10 inches	$\frac{3}{8}$ inch
1524	10 "	7 "	$\frac{1}{2}$ "	1530	12 "	$9\frac{1}{8}$ "	"
1525	9 "	6 "	"	1932	13 "	10 "	"
1526	$9\frac{1}{4}$ "	$7\frac{1}{4}$ "	"	1933	14 "	11 "	"
1527	$10\frac{1}{4}$ "	$7\frac{1}{8}$ "	"	1934	16 "	12 "	"
1528	11 "	8 "	"				

Other sizes made to order.

MANUFACTURED BY
LIBRARY BUREAU

DIVISION OF SPERRY RAND CORPORATION
Library Supplies of all Kinds

USGS LIBRARY - RESTON



3 1818 00082943 0